

Particle-Antiparticle Mixing, ε_K and the Unitarity Triangle in the Littlest Higgs Model

Andrzej J. Buras, Anton Poschenrieder and Selma Uhlig

Physik Department, Technische Universität München, D-85748 Garching, Germany

Abstract

We calculate the $K^0 - \bar{K}^0$, $B_{d,s}^0 - \bar{B}_{d,s}^0$ mixing mass differences ΔM_K , $\Delta M_{d,s}$ and the CP-violating parameter ε_K in the Littlest Higgs (LH) model. For f/v as low as 5 and the Yukawa parameter $x_L < 0.8$, the enhancement of ΔM_d amounts to at most 20%. Similar comments apply to ΔM_s and ε_K . The correction to ΔM_K is negligible. The dominant new contribution in this parameter range, calculated here for the first time, comes from the box diagrams with (W_L^\pm, W_H^\pm) exchanges and ordinary quarks that are only suppressed by the mass of W_H^\pm but do not involve explicit $\mathcal{O}(v^2/f^2)$ factors. This contribution is strictly positive. The explicit $\mathcal{O}(v^2/f^2)$ corrections to the SM diagrams with ordinary quarks and two W_L^\pm exchanges have to be combined with the box diagrams with a single heavy T quark exchange for the GIM mechanism to work. These $\mathcal{O}(v^2/f^2)$ corrections are found to be of the same order of magnitude as the (W_L^\pm, W_H^\pm) contribution but only for x_L approaching 0.8 they can compete with it. We point out that for $x_L > 0.85$ box diagrams with two T exchanges have to be included. Although formally $\mathcal{O}(v^4/f^4)$, this contribution is dominant for $x_L \approx 1$ due to non-decoupling of T that becomes fully effective only at this order. We emphasize, that the concept of the unitarity triangle is still useful in the LH model, in spite of the $\mathcal{O}(v^2/f^2)$ corrections to the CKM unitarity involving only ordinary quarks. We demonstrate the cancellation of the divergences in box diagrams that appear when one uses the unitary gauge for W_L^\pm and W_H^\pm .

1 Introduction

An attractive idea to solve the gauge hierarchy problem is to regard the electroweak Higgs boson as a pseudo-goldstone boson of a certain global symmetry that is broken spontaneously at a scale $\Lambda \sim 4\pi f \sim \mathcal{O}(10 \text{ TeV})$, much higher than the vacuum expectation value v of the standard Higgs doublet. Concrete realizations of this idea are the “Little Higgs” models [1]-[5] in which the Higgs field remains light, being protected by the approximate global symmetry from acquiring quadratically divergent contributions to its mass at the one-loop level. In models of this type new heavy particles are present, that analogously to supersymmetric particles allow to cancel the quadratic divergences in question. Reviews of the Little Higgs models can be found in [6].

One of the simplest models of this type is the “Littlest Higgs” model [4] (LH) in which, in addition to the Standard Model (SM) particles, new charged heavy vector bosons (W_H^\pm), a neutral heavy vector boson (Z_H), a heavy photon (A_H), a heavy top quark (T) and a triplet of heavy Higgs scalars ($\Phi^{++}, \Phi^+, \Phi^0$) are present. The details of this model including the Feynman rules have been worked out in [7] and the constraints from various processes, in particular from electroweak precision observables and direct new particles searches, have been extensively discussed in [7]-[13]. It has been found that except for the heavy photon A_H , that could still be as “light” as 500 GeV, the masses of the remaining particles are constrained to be significantly larger than 1 TeV.

The question then arises whether the Flavour Changing Neutral Current (FCNC) processes, such as particle-antiparticle mixings and various rare K and B decays, that played such an essential role in the construction of the SM, could further constrain the parameters of the LH model. This issue is particularly interesting because the mixing of the SM top quark (t) and of the heavier top (T) induces violation of the three generation unitarity of the CKM matrix at $\mathcal{O}(v^2/f^2)$ that is essential for a natural suppression of the FCNC processes (GIM mechanism) [14]. Moreover, as the mass of T must be larger than 1 TeV, interesting non-decoupling effects of this very heavy quark could play a role similar to the non-decoupling of t from FCNC processes that increases quadratically with m_t .

In the present paper we calculate the new particle contributions to $K^0 - \bar{K}^0$, $B_{d,s}^0 - \bar{B}_{d,s}^0$ mixings and to the CP violation parameter ε_K within the LH model [4]. We also address the unitarity triangle in the presence of the violation of the CKM unitarity at the $\mathcal{O}(v^2/f^2)$ level, pointing out that this triangle can be used in the LH model, provided the uncorrected CKM elements are used as basic parameters. The corresponding analysis of

rare K and B decays, that is more involved, will be presented elsewhere [15, 16].

We are not the first to address the question of FCNC processes within the LH model. In [17] the LH corrections to the decay $B \rightarrow X_s \gamma$ have been found to be small, while in [18] it has been pointed out that sizable effects could be present in $D^0 - \bar{D}^0$ mixing, where in contrast to processes involving external down quarks, FCNC transitions are already present at the tree level. Recently, in two interesting papers, Choudhury et al. [19, 20] analyzed the $B_d^0 - \bar{B}_d^0$ mass difference ΔM_d and the decay $K_L \rightarrow \pi^0 \nu \bar{\nu}$ within the model in question, finding a significant suppression of ΔM_d and a large enhancement of the branching ratio for $K_L \rightarrow \pi^0 \nu \bar{\nu}$ relative to the SM expectations.

Unfortunately our analysis of ΔM_d presented here does not confirm the findings of [19], both in sign and magnitude, for the same input parameters. Instead of a suppression of ΔM_d found by these authors, we find an *enhancement* in the full range of parameters considered but this enhancement amounts to at most 20% for $f/v \geq 5$, the masses of W_H^\pm , T and Φ^\pm larger than 1.5 TeV and the Yukawa parameter $x_L < 0.8$ (see (2.5)). The same comments apply to ΔM_s and ε_K . The corrections to ΔM_K are negligible. We conclude therefore that in view of non-perturbative uncertainties in ΔM_K , $\Delta M_{d,s}$ and ε_K it will be very difficult in this range of parameters to distinguish the LH expectations for these quantities from the SM ones. Consequently, in contrast to [19], we find that the constraints on LH model parameters coming from ΔM_d are for $x_L < 0.8$ substantially weaker than the ones coming from other processes [7]-[13]. On the other hand, as pointed out in [15] and below, for $x_L > 0.85$, where the non-decoupling effects of T enter at full strength, the LH corrections turn out to be larger, putting some constraints on the space of parameters [15].

The first difference between our analysis and the one of [19] is that we include the box diagrams with the ordinary quarks, one W_L^\pm and one W_H^\pm exchanges that enter ΔM_d at $\mathcal{O}(1)$ in the couplings and are only suppressed by the mass of W_H^\pm relatively to the usual box diagrams with two W_L^\pm exchanges. Surprisingly the authors of [19] omitted this contribution although they took into account partially the $\mathcal{O}(v^2/f^2)$ corrections to the box diagrams with (W_L^\pm, W_H^\pm) exchanges. While we find the latter contribution totally negligible, the former turns out to be the dominant one for $x_L < 0.7$ and, being positive, governs the sign of the full effect.

The second important contribution, also considered in [19], are the $\mathcal{O}(v^2/f^2)$ effects related to the modification of the vertices in the usual box diagrams with ordinary quarks and two W_L^\pm exchanges. As emphasized in [19, 20], due to the violation of the CKM unitarity at $\mathcal{O}(v^2/f^2)$ these corrections have to be considered simultaneously with box diagrams involving single T for the GIM mechanism to be effective. We find that these $\mathcal{O}(v^2/f^2)$ contributions can have both signs depending on the input parameters but in

a large region of parameters considered they interfere constructively with the diagrams with (W_L^\pm, W_H^\pm) exchanges, increasing the enhancement of ΔM_d , ΔM_s and ε_K . The general structure of this contribution presented, before the use of the GIM mechanism, in [19] is equal to ours but their final numerical result indicates that the sign of this contribution and also its magnitude differ from our findings.

The third contribution, not considered in [19], comes from box diagrams with two T exchanges. Although formally $\mathcal{O}(v^4/f^4)$ this contribution increases linearly with $x_T = m_T^2/M_W^2$ and with $x_T = \mathcal{O}(f^2/v^2)$ constitutes effectively an $\mathcal{O}(v^2/f^2)$ correction. For the Yukawa coupling parameter $x_L \approx 1$, this contribution turns out to be more important than the remaining $\mathcal{O}(v^2/f^2)$ corrections. In particular it is larger than the $\mathcal{O}(v^2/f^2)$ contribution of box diagrams with a single T exchange discussed above that increases only logarithmically with x_T .

We are aware of the fact that with increasing m_T also one-loop corrections to the SM Higgs mass increase. Typically for $m_T \geq 6$ TeV a fine-tuning of at least 1% has to be made in order to keep m_H below 200 GeV [21, 22]. As roughly $f/v \geq 8$ is required by electroweak precision studies [7]-[13], the non-decoupling effects of T considered here can be significant and simultaneously consistent with these constraints only in a narrow range of f/v . But these bounds are clearly model dependent [23, 24] and we will consider the range $5 \leq f/v \leq 15$ and $x_L \leq 0.95$ for completeness.

The fourth non-negligible correction, not considered in [19], is the one related to the use of the standard value of the Fermi constant G_F that enters quadratically in all the quantities considered here. In order to include this correction in the evaluation of ΔM_i and ε_K , we calculate the amplitude for the muon decay in the LH model at the tree level. The resulting additional correction to $\Delta M_{d,s}$, ε_K , and ΔM_K amounts to at most a few percent but being negative it reduces the enhancements slightly.

Finally, we find that the contribution of the heavy scalar Φ^\pm can be neglected for all practical purposes as it is well below 1% of the full result for all quantities considered.

On the technical side, we have performed the calculations in the unitary gauge for the W_L^\pm and W_H^\pm propagators which has the nice virtue that only exchanges of physical particles have to be considered. On the other hand in contrast to a R_ξ gauge with a finite gauge parameter ξ , the box diagrams in the unitary gauge are divergent, both in the SM and the LH model. As already stated in [19] these divergences cancel when the unitarity of the CKM matrix in the SM is used and the contribution of the heavy T is included in the LH model at $\mathcal{O}(v^2/f^2)$. As the authors of [19] did not demonstrate this explicitly, we will show this cancellation in Section 3. This exercise turned out to be very instructive. Indeed, the cancellation of the divergences in box diagrams at $\mathcal{O}(v^2/f^2)$ takes only place when the vertex involving $W_L^\pm(W_H^\pm)$ and $\bar{T}d_i$ with d_i being ordinary down quarks, has

the same factor i as the vertex involving the weak gauge bosons and $\bar{t}d_i$. This is not fully evident from the widely used Feynman rules for the LH model given in [7] that uses different phase conventions for the T and t fields.

Our paper is organized as follows. In Section 2 we recall very briefly those elements of the LH model that are necessary for the discussion of our calculation. As a preparation for subsequent sections we calculate the amplitude for the muon decay in the LH model at the tree level and we investigate whether the usual determination of the CKM elements, not involving the top quark, by means of tree level decays could be affected by the LH contributions in a non-negligible manner. This turns out not to be the case. Performing analogous exercise for the tree level decay of the top quark into b quark and leptons, we demonstrate how in principle the violation of the three generation CKM unitarity in the LH model could be detected experimentally. Finally we emphasize that working with uncorrected CKM elements as basic parameters, allows to display the effects of the LH contributions in the usual $(\bar{\varrho}, \bar{\eta})$ plane [25, 26]. They manifest themselves primarily in the modification of the angle γ and the side R_t in such a manner that the angle β and the side R_b remain unchanged. While this analysis is partly academic in view of the smallness of corrections found here, it could turn out to be useful in other processes and other Little Higgs models in which larger effects in FCNC processes could be present.

In Section 3 we demonstrate explicitly the cancellation of the divergences in the box diagrams calculated in the unitary gauge. In Section 4 we discuss briefly our calculation for $x_L \leq 0.8$ and present analytic expressions for the relevant contributions in this parameter region. For completeness we give in Appendix A the results for the $\mathcal{O}(v^2/f^2)$ corrections to box diagrams with (W_L^\pm, W_H^\pm) exchanges and the contribution of the scalars Φ^\pm . It will be clear from these formulae that these corrections are fully negligible. In Section 5 we discuss the non-decoupling effects of T , that are already visible in the box diagrams with a single T exchange considered in Section 4, but are fully effective only in the region $x_L \approx 1$ in which the dominant correction $\mathcal{O}(v^4/f^4)$, the box diagram with two T exchanges, has to be taken into account.

In Section 6 we present the numerical analysis of the formulae of Sections 4 and 5. In Section 7 we briefly discuss the issue of QCD corrections within the LH model. For scales $\mu \leq \mu_t = \mathcal{O}(m_t)$ they are the same as in the SM but the contribution of QCD corrections from higher scales are different. In view of the smallness of the new contributions and the theoretical uncertainties involved, it is clearly premature to compute these additional QCD corrections. Still our discussion indicates that they should further suppress the LH contributions. A brief summary of our paper is given in Section 8.

2 Aspects of the Littlest Higgs Model

2.1 Preliminaries

Let us first recall certain aspects of the LH model that are relevant for our work. The full exposition can be found in the original paper [4] and in [7], where Feynman rules for the LH model have been worked out. We will follow the notations of [7], although due to different phase conventions for the t and T fields, our rules for the vertices $W_L^\pm \bar{T} d_j$ and $W_H^\pm \bar{T} d_j$ differ by a crucial factor i as discussed below.

The new particles that enter the calculations in the present paper are W_H^\pm , T and Φ^\pm . To the order in v/f considered, their masses and their interactions with ordinary quarks and leptons can be entirely expressed in terms of

$$m_t \equiv \bar{m}_t(m_t) = 168.1 \text{ GeV}, \quad M_{W_L^\pm} = 80.4 \text{ GeV}, \quad M_H \geq 115 \text{ GeV} \quad (2.1)$$

and the following three new parameters of the LH model

$$f/v, \quad s, \quad x_L. \quad (2.2)$$

Using the formulae in [7] we find

$$m_T = \frac{f}{v} \frac{m_t}{\sqrt{x_L(1-x_L)}}, \quad M_{W_H^\pm} = \frac{f}{v} \frac{M_{W_L^\pm}}{sc}, \quad M_{\Phi^\pm} \geq \sqrt{2} M_H \frac{f}{v}. \quad (2.3)$$

As Φ^\pm will play a negligible role in this analysis, we need only to know its lower bound.

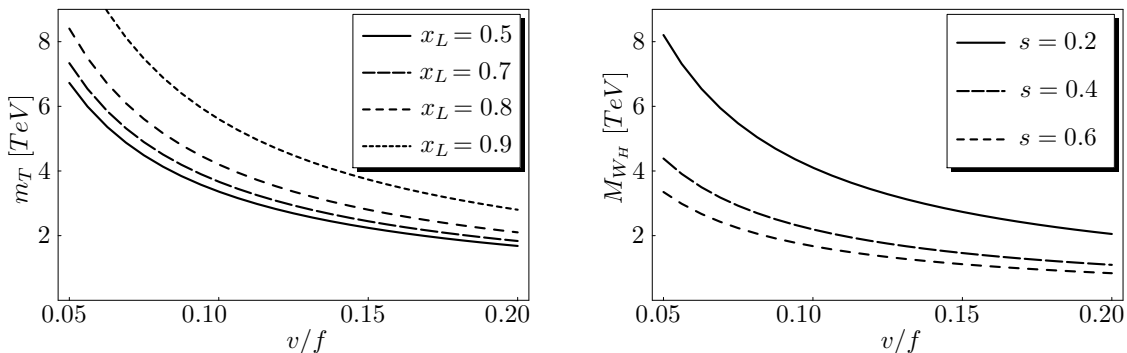


Figure 1: The masses of the heavy top quark T and the heavy W_H boson as functions of v/f for different values of x_L and s .

We recall that $v = 246$ GeV is the vacuum expectation value of the standard Higgs doublet. The parameters s and c are the sine and the cosine of the mixing angle between $SU(2)_1$ and $SU(2)_2$ gauge bosons of the original gauge symmetry group

$[SU(2)_1 \otimes U(1)_1] \otimes [SU(2)_2 \otimes U(1)_2]$ that is spontaneously broken down to the SM gauge group. The resulting $SU(2)_L$ gauge coupling g is then related to the g_i couplings of the $SU(2)_i$ groups through

$$g = sg_1 = cg_2, \quad c^2 = 1 - s^2. \quad (2.4)$$

Finally,

$$x_L = \frac{\lambda_1^2}{\lambda_1^2 + \lambda_2^2}, \quad (2.5)$$

where λ_1 is the Yukawa coupling in the (t, T) sector and λ_2 parametrizes the mass term of T . The parameter x_L enters the sine of the t - T mixing which is simply given by $x_L v/f$. As we will see below, the parameter x_L describes together with v/f the size of the violation of the three generation CKM unitarity and is also crucial for the gauge interactions of the heavy T quark with the ordinary down quarks. λ_i are expected to be $\mathcal{O}(1)$ with [7]

$$\lambda_i \geq \frac{m_t}{v}, \quad \text{or} \quad \frac{1}{\lambda_1^2} + \frac{1}{\lambda_2^2} \approx \left(\frac{v}{m_t}\right)^2 \quad (2.6)$$

so that within a good approximation

$$\lambda_1 = \frac{m_t}{v} \frac{1}{\sqrt{1-x_L}}, \quad \lambda_2 = \frac{m_t}{v} \frac{1}{\sqrt{x_L}}. \quad (2.7)$$

x_L can in principle vary in the range $0 < x_L < 1$. For $x_L \approx 0$ and $x_L \approx 1$, the mass m_T becomes very large. This is seen in Fig. 1, where we show the masses of the heavy top quark T and the heavy W_H boson as functions of v/f for different values of x_L and s . The fact that for $x_L \approx 1$ the Yukawa coupling λ_1 becomes large is responsible for the non-decoupling of T at fixed v/f as discussed in Section 5.

2.2 Fermion-Gauge Boson Interactions

In table VIII of [7] Feynman rules for the vertices involving W_L^\pm , W_H^\pm and the quarks have been given. We repeat them except that we introduce additional i factors in the rules involving the heavy T quark that we will discuss below. We have then

$$W_L^{+\mu} \bar{u}_i d_j = i \frac{g_2}{2\sqrt{2}} V_{ij} \left[1 - a \frac{v^2}{f^2} \right] \gamma_\mu (1 - \gamma_5) \quad (u_i = u, c) \quad (2.8)$$

$$W_L^{+\mu} \bar{t} d_j = i \frac{g_2}{2\sqrt{2}} V_{tj} \left[1 - \left(\frac{1}{2} x_L^2 + a \right) \frac{v^2}{f^2} \right] \gamma_\mu (1 - \gamma_5) \quad (2.9)$$

$$W_L^{+\mu} \bar{T} d_j = i \frac{g_2}{2\sqrt{2}} V_{tj} x_L \frac{v}{f} \gamma_\mu (1 - \gamma_5) \quad (2.10)$$

and

$$W_H^{+\mu} \bar{u}_i d_j = -i \frac{g_2}{2\sqrt{2}} V_{ij} \frac{c}{s} \left[1 + b \frac{v^2}{f^2} \right] \gamma_\mu (1 - \gamma_5) \quad (u_i = u, c) \quad (2.11)$$

$$W_H^{+\mu} \bar{t} d_j = -i \frac{g_2}{2\sqrt{2}} V_{tj} \frac{c}{s} \left[1 - \left(\frac{1}{2} x_L^2 - b \right) \frac{v^2}{f^2} \right] \gamma_\mu (1 - \gamma_5) \quad (2.12)$$

$$W_H^{+\mu} \bar{T} d_j = -i \frac{g_2}{2\sqrt{2}} V_{tj} \frac{c}{s} x_L \frac{v}{f} \gamma_\mu (1 - \gamma_5) \quad (2.13)$$

where

$$a = \frac{1}{2} c^2 (c^2 - s^2), \quad b = \frac{1}{2} s^2 (c^2 - s^2). \quad (2.14)$$

The $\mathcal{O}(v^2/f^2)$ corrections to the W_H^\pm couplings, not contained in table VIII of [7], follow from equation (A51) of the latter paper. The Feynman rules for the leptons are given by (2.8) and (2.11) with $V_{ij} = 1$.

Here V_{ij} are the usual CKM parameters, denoted by V_{ij}^{SM} in [7]. They satisfy the usual unitarity relations. In particular we have

$$\lambda_u + \lambda_c + \lambda_t = 0, \quad \lambda_i = V_{ib}^* V_{id}. \quad (2.15)$$

As seen in (2.9) and (2.12) at $\mathcal{O}(v^2/f^2)$ there is a disparity between the $W_L^{+\mu} (W_H^{+\mu})$ couplings of t and of the lighter quarks u and c to the down quarks. This is related to the fact that in the LH model the elements V_{ij} are generalized to [7, 18]

$$\hat{V}_{ij} = V_{ij} \quad \text{for} \quad i = u, c \quad (2.16)$$

and

$$\hat{V}_{tj} = V_{tj} \left(1 - \frac{x_L^2 v^2}{2 f^2} \right), \quad \hat{V}_{Tj} = V_{tj} \frac{v}{f} x_L \quad (2.17)$$

and include now also the heavy T .

We observe that the $\mathcal{O}(v^2/f^2)$ corrections to V_{tj} in (2.17) violate the usual CKM unitarity relations like the one in (2.15) but the generalized unitarity relation [18]

$$\hat{\lambda}_u + \hat{\lambda}_c + \hat{\lambda}_t + \hat{\lambda}_T = 0, \quad \hat{\lambda}_i = \hat{V}_{ib}^* \hat{V}_{id}, \quad (2.18)$$

that includes also the heavy T is clearly satisfied at $\mathcal{O}(v^2/f^2)$.

The Feynman rules in (2.8)–(2.13) are the same as in [7] except for the additional i factors in (2.10) and (2.13). The absence of these factors in table VIII of [7] is related to the fact that with the i factors present in the fermion mass terms in equation (A43) of that paper the parameter s_L in (A44) of [7] is an imaginary quantity and $s_L^2 + c_L^2 = 1$ is not satisfied. Redefining appropriately the quark fields, s_L changes to $is_L = s_L^{\text{new}}$, and $(s_L^{\text{new}})^2 + c_L^2 = 1$. The factor i is now present in (2.10) and (2.13) as it should be. In the

case of box diagrams with a single T exchange the contribution of this heavy quark to ΔM_i and ε_K has wrong sign if i is not present in (2.10) and (2.13) and the divergences in box diagrams calculated in the unitary gauge do not cancel. We will return to this point below.

2.3 Determination of the CKM Parameters

It is of interest to ask whether the presence of the contributions from new particles could have an effect on the numerical values of the CKM elements not involving t that are usually determined in tree level decays.

In order to address this issue we have to study first the muon decay that is usually used to measure the Fermi constant G_F . It is sufficient to look at the tree level and include only $\mathcal{O}(v^2/f^2)$ corrections. In the LH model, in addition to the W_L^\pm exchange also the W_H^\pm exchange has to be taken into account. The contribution of Φ^\pm is negligible as it is suppressed both by the v/f factors in the vertices [7] and its large mass.

The Feynman rules for the leptons are identical to the ones for the lighter quarks except for the CKM factors. Calculating tree level exchange of W_L^\pm with $\mathcal{O}(v^2/f^2)$ corrections taken into account and adding to it the tree level exchange of W_H^\pm without these corrections gives the standard amplitude for the muon decay with G_F replaced by

$$G_F^{\text{eff}} = G_F \left(1 + c^2 s^2 \frac{v^2}{f^2} \right), \quad \frac{G_F}{\sqrt{2}} = \frac{g^2}{8M_{W_L}^2}. \quad (2.19)$$

To this end we have used the formula for $M_{W_H^\pm}$ in (2.3). It is G_F^{eff} that should be identified with the G_F usually measured in the muon decay.

With this information at hand we can now calculate the amplitudes for the relevant tree level semileptonic decays in the LH model that are used to determine the CKM elements. Proceeding as in the case of the muon decay and redefining G_F to G_F^{eff} we find that:

- The numerical values of all the CKM elements not involving the top quark are not modified at this level.
- The numerical values of the CKM elements V_{tb} , V_{ts} , V_{td} determined in tree level decays of the top quark to lighter quarks, would also lead to the same results as in the SM but this time for \hat{V}_{tb} , \hat{V}_{ts} , \hat{V}_{td} in (2.17), respectively.

This exercise shows immediately how the violation of the three generation CKM unitarity in the LH model could be in principle discovered by experimentalists in semileptonic decays of t to b . Measuring V_{tb} , but not realizing that what is really measured

is \hat{V}_{tb} , would give the value of V_{tb} that is smaller than the true value. This would result in the violation of the unitarity relation

$$|V_{ub}|^2 + |V_{cb}|^2 + |V_{tb}|^2 = 1 \quad (2.20)$$

with the l.h.s smaller than unity. Realizing that \hat{V}_{tb} and not V_{tb} has been measured and using (2.17) to find the true value of V_{tb} , would allow to satisfy (2.20).

2.4 Unitarity Triangle in the LH Model

In view of the $\mathcal{O}(v^2/f^2)$ corrections to the ordinary CKM elements, as given in (2.17), the unitarity relation for the physical CKM elements \hat{V}_{ij} involving only ordinary quarks is no longer satisfied

$$\hat{\lambda}_u + \hat{\lambda}_c + \hat{\lambda}_t \neq 0. \quad (2.21)$$

It would appear then that in the LH model the usual analysis of the unitarity triangle (UT) should be generalized to a unitarity quadrangle based on the relation (2.18). A discussion in this spirit has been presented in a different context in [18].

Here we would like to emphasize that the usual analysis of the UT remains still valid in the LH model, provided we use as basic parameters the elements V_{ij} that clearly satisfy the unitarity relation (2.15). In this formulation the v^2/f^2 corrections to the CKM elements in (2.17) are explicitly seen and contribute manifestly to various amplitudes and branching ratios that are written in terms of V_{ij} and not \hat{V}_{ij} . The effect of the $\mathcal{O}(v^2/f^2)$ corrections in the CKM elements involving the top quark will be then felt together with other corrections in the modification of the numerical values of the sides and angles of the UT relative to the ones obtained in the SM.

Clearly, it is possible to proceed differently and express all amplitudes and branching ratios in terms of \hat{V}_{ij} and not V_{ij} . In this formulation the $\mathcal{O}(v^2/f^2)$ corrections to the CKM matrix elements will be absorbed into \hat{V}_{ij} and the explicit $\mathcal{O}(v^2/f^2)$ corrections will differ from the ones in the formulation in terms of V_{ij} . But as the values of \hat{V}_{ij} differ from V_{ij} , as seen explicitly in (2.17), the final result for physical quantities will be the same up to corrections of $\mathcal{O}(v^4/f^4)$.

This discussion is fully analogous to the ones of the definition of the QCD coupling constant and the definition of parton distributions in deep inelastic scattering. We are confident that in the context of the LH model, the variables V_{ij} are superior to \hat{V}_{ij} and we will use them in what follows. This allows, in particular, to exhibit the impact of LH effects on various processes in the $(\bar{\varrho}, \bar{\eta})$ plane.

3 GIM Mechanism and Unitary Gauges

3.1 Preliminaries

The amplitudes for FCNC processes in the SM and various extensions like supersymmetry and models with extra dimensions, are usually calculated in the Feynman gauge or R_ξ gauges for the gauge bosons. This requires the inclusion of the corresponding Goldstone bosons in order to obtain gauge independent result. In models with larger gauge groups, that are spontaneously broken down to the SM group, it is more convenient to work in the unitary gauge, thus avoiding the calculation of many diagrams with Goldstone bosons. On the other hand, due to different high momentum behaviour of gauge boson propagators, even box diagrams are divergent in this gauge. These divergences must then cancel each other after the unitarity of the CKM matrix has been used. To our knowledge no explicit demonstration of the cancellation of these divergences has been presented in the literature. We will first illustrate this within the SM and subsequently in the LH model where due to the violation of three generation unitarity by $\mathcal{O}(v^2/f^2)$ corrections, the cancellation in question is more involved.

3.2 The Standard Model

In the SM the effective Hamiltonian for $B_d^0 - \bar{B}_d^0$ mixing neglecting QCD corrections can be written before the use of the CKM unitarity as follows

$$H_{\text{eff}}(\Delta B = 2) = \frac{G_F^2}{16\pi^2} M_{W_L^\pm}^2 \sum_{i,j=u,c,t} \lambda_i \lambda_j F(x_i, x_j; W_L) (\bar{b}d)_{V-A} (\bar{b}d)_{V-A} \quad (3.1)$$

where

$$\lambda_i = V_{ib}^* V_{id}, \quad x_i = \frac{m_i^2}{M_{W_L^\pm}^2}. \quad (3.2)$$

The functions $F(x_i, x_j; W_L)$ result up to an overall factor from box diagram with two W_L^\pm and two quarks (i, j) exchanges.

The unitarity of the CKM matrix implies the relation (2.15). Inserting $\lambda_u = -\lambda_c - \lambda_t$ into (3.1) and keeping only the term proportional to λ_t^2 one finds

$$H_{\text{eff}}(\Delta B = 2) = \frac{G_F^2}{16\pi^2} M_{W_L^\pm}^2 \lambda_t^2 S_0(x_t) (\bar{b}d)_{V-A} (\bar{b}d)_{V-A}, \quad (3.3)$$

where

$$S_0(x_t) = F(x_t, x_t; W_L) + F(x_u, x_u; W_L) - 2F(x_u, x_t; W_L). \quad (3.4)$$

Similarly the coefficient of $2\lambda_c\lambda_t$ is given by

$$S_0(x_c, x_t) = F(x_c, x_t; W_L) + F(x_u, x_u; W_L) - F(x_u, x_c; W_L) - F(x_u, x_t; W_L). \quad (3.5)$$

In any R_ξ gauge for the W_L^\pm propagator the functions F are finite but contain x_i -independent terms that, when present, would be disastrous in particular for the evaluation of the $K_L - K_S$ mass difference ΔM_K [27]. Such terms evidently cancel in (3.4) and (3.5) and in an analogous expression for $S_0(x_c)$, that to an excellent approximation, is given then by x_c , providing the necessary suppression of ΔM_K in accordance with experimental findings.

In the unitary gauge the functions F are divergent quantities with the divergence given up to an overall x_i -independent factor by

$$F_{\text{div}}(x_i, x_j; W_L) \sim \frac{1}{\varepsilon}(x_i + x_j + \text{const.}) \quad (3.6)$$

with ε defined through $D = 4 - 2\varepsilon$. It is evident that these singularities cancel in the expressions (3.4) and (3.5). We have verified that the remaining terms reproduce the known expressions for $S_0(x_t)$ and $S_0(x_c, x_t)$ that are given in Appendix B.

For pedagogical reasons it is instructive to demonstrate how these divergences disappear when the use of the relations (3.4) and (3.5) is already done at the level of the integrand so that the use of the dimensional regularization can be avoided altogether. This is in fact useful when the calculations are done by hand although immaterial when computer software for analytical calculations is used.

In the process of the evaluation of the functions $F(x_i, x_j; W_L)$ in the unitary gauge, two divergent integrals corresponding respectively to $g_{\alpha\beta}k_\mu k_\nu$ and $k_\alpha k_\beta k_\mu k_\nu$ factors appear:

$$I_n(x_i, x_j) = \int_0^\infty dr \frac{r^{2+n}}{(r+x_i)(r+x_j)(r+1)^2} \quad n = 1, 2. \quad (3.7)$$

Inserting these integrals into (3.4) results in finite integrals

$$I_n^{\text{GIM}}(x_t, x_t) = x_t^2 \int_0^\infty dr \frac{r^n}{(r+x_t)^2(r+1)^2} \quad n = 1, 2 \quad (3.8)$$

with an analogous result for $I_n^{\text{GIM}}(x_c, x_t)$. It is remarkable that the GIM mechanism reduces the power in the numerator by two.

3.3 Littlest Higgs Model

As discussed above, at $\mathcal{O}(v^2/f^2)$ the CKM matrix involving only the usual three generations of quarks is no longer unitary. Consequently when $\mathcal{O}(v^2/f^2)$ corrections to the $W_L^\pm \bar{u}_i d_j$ vertices are included and only the exchanges of ordinary quarks are taken into account the functions $S_0(x_t)$ and $S_0(x_c, x_t)$ are divergent at $\mathcal{O}(v^2/f^2)$ even if the relation (2.15), still valid at $\mathcal{O}(1)$ in the LH model, is used. This leftover divergence is then cancelled by box diagrams involving a single T quark in place of an ordinary quark. At $\mathcal{O}(v^4/f^4)$ the inclusion of box diagrams with two T quarks becomes necessary.

The basic formula that guarantees the cancellation of the quadratic divergences in the LH model is the generalized unitarity relation (2.18). For this relation to be effective in the evaluation of the box diagrams and also penguin diagrams it is essential that the Feynman rules in (2.10) and (2.13) contain the factor i , that in fact is not present in the corresponding rules in Table VIII of [7]. We have discussed this point in Section 2. In the case of box diagrams with a single T exchange, the omission of this i factor would give the wrong sign for the T contribution and the divergences coming from diagrams with ordinary quarks would not be cancelled. We will return to this point when presenting our results in the subsequent section.

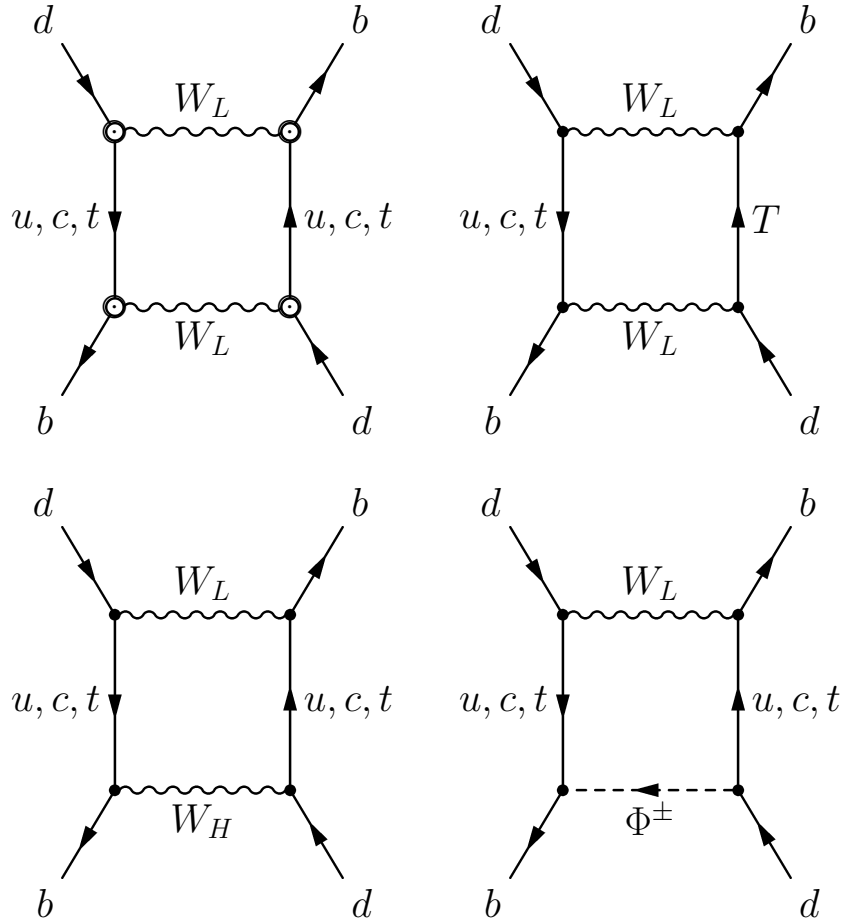


Figure 2: Contributing box diagrams at $\mathcal{O}(v^2/f^2)$

4 Analytic Results

In this section we will present analytic results for the $\mathcal{O}(v^2/f^2)$ corrections to ΔM_K , $\Delta M_{d,s}$ and the CP-violating parameter ε_K in the LH model.

The effective Hamiltonian for $\Delta S = 2$ transitions can be written as follows

$$H_{\text{eff}} = \frac{G_F^2}{16\pi^2} M_{W_L^\pm}^2 [\lambda_c^2 \eta_1 S_c + \lambda_t^2 \eta_2 S_t + 2\lambda_c \lambda_t \eta_3 S_{tc}] (\bar{s}d)_{V-A} (\bar{s}d)_{V-A}, \quad (4.1)$$

where $\lambda_i = V_{is}^* V_{id}$. In the case of $B_d^0 - \bar{B}_d^0$ mixing and $B_s^0 - \bar{B}_s^0$ mixing the formula (3.3) applies with $S_0(x_t)$ replaced by $\eta_B S_t$. The factors η_i are QCD corrections [29, 30, 31] to which we will return in Section 7.

Using (4.1) one obtains the following expressions for quantities considered in this paper [28]:

$$\varepsilon_K = C_\varepsilon \hat{B}_K \text{Im} \lambda_t \{ \text{Re} \lambda_c [\eta_1 S_c - \eta_3 S_{ct}] - \text{Re} \lambda_t \eta_2 S_t \} e^{i\pi/4}, \quad (4.2)$$

$$\Delta M_q = \frac{G_F^2}{6\pi^2} \eta_B m_{B_q} (\hat{B}_{B_q} F_{B_q}^2) M_{W_L}^2 S_t |\lambda_t|^2, \quad q = d, s, \quad (4.3)$$

where the numerical constant $C_\varepsilon = 3.837 \cdot 10^4$, F_{B_q} is the B_q meson decay constant, \hat{B}_i are non-perturbative parameters and η_B stands for short distance QCD correction that slightly differs from η_2 in (4.1) [30, 31].

As discussed in Section 2, it is convenient to work directly with λ_i rather than $\hat{\lambda}_i$ and include the effects of the corrections to the CKM matrix in the functions S_i and S_{ij} . We decompose therefore the functions S_i and S_{ij} into known SM contributions and the corrections coming from new particles in the LH model as follows

$$S_t = S_0(x_t) + \Delta S_t, \quad (4.4)$$

$$S_{ct} = S_0(x_c, x_t) + \Delta S_{ct}, \quad (4.5)$$

$$S_c = S_0(x_c) + \Delta S_c. \quad (4.6)$$

The diagrams contributing to the functions ΔS_i at $\mathcal{O}(v^2/f^2)$ are shown in Fig. 2. The circles around the vertices in the first diagram that involves only SM particles indicate $\mathcal{O}(v^2/f^2)$ corrections to the W_L^\pm vertices. Explicit expressions are given in (2.8) and (2.9). No such corrections have to be included in the last two diagrams with W_H^\pm and Φ^\pm , exchanges because of the large masses of these particles. The case of the second diagram with T is different due to the non-decoupling of T . We will return to this point in the next section.

This discussion shows that the contribution of the scalars Φ^\pm is much smaller than the remaining contributions as the last diagram in Fig. 2 is suppressed by both v^2/f^2 in the vertices involving Φ^\pm and the large mass M_{Φ^\pm} . We have confirmed this expectation

through an explicit calculation. We therefore omit this contribution in what follows but for completeness give the analytic expression for it in Appendix A.

Similarly the $\mathcal{O}(v^2/f^2)$ corrections to the third diagram, that involve necessarily also a single T exchange like in the second diagram, give contributions that can be neglected in comparison with the first three diagrams. For completeness we give the analytic expression for these corrections in Appendix A.

The expressions for ΔS_i and ΔS_{ij} that are obtained from the first three diagrams of Fig. 2 are then given as follows:

$$\Delta S_t = -4 \frac{v^2}{f^2} \left[a S_0(x_t) + \frac{1}{2} x_L^2 P_1(x_t, x_T) \right] + 2 \frac{c^2}{s^2} P_3(x_t, y) \quad (4.7)$$

$$\Delta S_{ct} = -4 \frac{v^2}{f^2} \left[a S_0(x_c, x_t) + \frac{1}{4} x_L^2 P_2(x_c, x_t, x_T) \right] + 2 \frac{c^2}{s^2} P_4(x_c, x_t, y) \quad (4.8)$$

with ΔS_c obtained from (4.7) through the substitution $t \rightarrow c$ and setting $x_L = 0$. The parameters x_L and a are defined in (2.5) and (2.14), respectively. Moreover

$$x_i = \frac{m_i^2}{M_{W_L^\pm}^2}, \quad y = \frac{M_{W_H^\pm}^2}{M_{W_L^\pm}^2}. \quad (4.9)$$

Explicit expressions for the functions S_0 and P_i are given in Appendix B. It turns out that in the range of parameters considered, the four functions involved can be approximated within an excellent accuracy by

$$P_1(x_t, x_T) = -\frac{x_t}{4} (\log x_T - 1.57) \quad (4.10)$$

$$P_2(x_c, x_t, x_T) = -\frac{x_c}{4} (\log x_T + 0.65) \quad (4.11)$$

$$P_3(x_t, y) = \frac{x_t}{y} \quad (4.12)$$

$$P_4(x_c, x_t, y) = \frac{x_c}{y} \log \frac{x_t}{x_c}, \quad (4.13)$$

where the numerical factors correspond to $m_t = 168.1$ GeV and $m_c = 1.3$ GeV. However, in our numerical analysis, we will use the exact expressions.

The expressions for the functions P_i in terms of the functions F resulting from individual diagrams are given as follows:

$$P_1(x_t, x_T) = F(x_t, x_t; W_L) + F(x_u, x_T; W_L) - F(x_t, x_T; W_L) - F(x_u, x_t; W_L) \quad (4.14)$$

$$P_2(x_c, x_t, x_T) = F(x_c, x_t; W_L) + F(x_u, x_T; W_L) - F(x_c, x_T; W_L) - F(x_u, x_t; W_L) \quad (4.15)$$

$$P_3(x_t, y) = F(x_t, x_t, y; W_L, W_H) + F(x_u, x_u, y; W_L, W_H) - 2F(x_t, x_u, y; W_L, W_H) \quad (4.16)$$

$$\begin{aligned}
P_4(x_c, x_t, y) &= F(x_c, x_t, y; W_L, W_H) + F(x_u, x_u, y; W_L, W_H) \\
&\quad - F(x_c, x_u, y; W_L, W_H) - F(x_t, x_u, y; W_L, W_H)
\end{aligned}
\tag{4.17}$$

As discussed in Section 3 each contribution in (4.14)–(4.17) is divergent in the unitary gauge but these divergences are absent in P_i . For this to happen the signs in front of the functions having the argument x_T must be as given above. This is only achieved with the i factor in the rules (2.10) and (2.13). Removing i from these rules would imply opposite signs in front of the functions involving T in (4.14)–(4.15) and no cancellation of divergences. This is evident from (3.6).

The results in (4.7) and (4.8) do not include the correction related to G_F that has been given in (2.19). Rewriting (4.1) in terms of G_F^{eff} results in the replacement

$$a \rightarrow a_{\text{eff}} = a + \frac{1}{2}c^2s^2 = \frac{1}{2}c^4.
\tag{4.18}$$

This correction slightly suppresses the enhancements of S_t and S_{ct} .

The formulae (4.7) - (4.18) and the analytic expressions for the functions P_i in Appendix B are the main results of this section.

5 Non-Decoupling Effects of the Heavy T

5.1 Preliminaries

In the previous section we have seen that box diagrams including simultaneously either W_H^\pm or Φ^\pm and explicit $\mathcal{O}(v^2/f^2)$ corrections in the vertices could be neglected for all practical purposes. Effectively they are $\mathcal{O}(v^4/f^4)$ with the additional suppression factor $\mathcal{O}(v^2/f^2)$ coming from the heavy gauge boson or scalar propagator.

This rule does not apply to the box diagram with the single T exchange in Fig. 2. Indeed as seen in (4.10) the contribution of this diagram increases logarithmically with x_T , rather than being suppressed by a heavy T quark propagator.

In order to understand this particular behaviour of diagrams involving T let us recall the known fact, that in the SM the FCNC processes are dominated by the contributions of top quark exchanges in box and penguin diagrams [28, 32, 33]. This dominance originates in the large mass m_t of the top quark and in its non-decoupling from low energy observables due to the corresponding Yukawa coupling that is proportional to m_t . In the evaluation of box and penguin diagrams in the Feynman-t'Hooft gauge this decoupling is realized through the diagrams with internal fictitious Goldstone boson and top quark exchanges. The couplings of Goldstone bosons to the top quark, being proportional to m_t , remove the suppression of the diagrams in question due to top quark

propagators so that at the end the box and penguin diagrams increase with increasing m_t . In the unitary gauge, in which fictitious Goldstone bosons are absent, this behaviour originates from the longitudinal $(k_\mu k_\mu/M_W^2)$ component of the W^\pm -propagators.

In particular, in the case of $B_{d,s}^0 - \bar{B}_{d,s}^0$ mixing and ε_K discussed here, the function $S_0(x_t)$ in (3.4) has the following large m_t behaviour

$$S_0(x_t) \rightarrow \frac{x_t}{4}. \quad (5.1)$$

Yet, with $x_t \approx 4.4$, this asymptotic formula is a very poor approximation of the true value $S_0(x_t) = 2.42$.

In the case of the Littlest Higgs model, the corresponding variable x_T is at least 400 and the asymptotic formula (4.10) is an excellent approximation of the exact expression for $P_1(x_t, x_T)$. The question then arises, whether this formula is an adequate description of the large m_T limit that as seen in (2.3) at fixed f/v corresponds to $x_L \approx 1$. As seen in (2.7) in this limit the Yukawa coupling λ_1 becomes large implying non-decoupling of T . Here we want to point out that in this limit also the $\mathcal{O}(v^4/f^4)$ contributions involving the T quark represented dominantly by box diagrams with two T exchanges must also be taken into account. In fact for $x_L \geq 0.95$ these $\mathcal{O}(v^4/f^4)$ corrections turn out to be the dominant correction in the LH model to the SM result for S_t . A short summary of the results obtained here appeared very recently in [15]. Here we present the details of these investigations.

5.2 Box Diagrams with Two T Exchanges

Returning to the results of the previous section, let us note that all contributions calculated there have a characteristic linear behaviour in x_t that signals the non-decoupling of the ordinary top quark. However, the corresponding non-decoupling of T is only logarithmic. This is related to the fact that with the $W_L^\pm \bar{T} d_j$ coupling being $\mathcal{O}(v/f)$ only box diagrams with a single T exchange (see Fig. 2) contribute at $\mathcal{O}(v^2/f^2)$. Similarly to the SM box diagrams with a single t exchange, that increase as $\log x_t$, the T contribution in the LH model increases only as $\log x_T$.

Yet, as discussed in [15], for $x_L \approx 1$ at fixed v/f , the $\log x_T$ behaviour of the T contribution found in the previous Section does not give a proper description of the non-decoupling of T . Indeed in this limit also the box diagram with two T exchanges given in Fig. 3 has to be considered. Although formally $\mathcal{O}(v^4/f^4)$, this contribution increases linearly with x_T and with $x_T = \mathcal{O}(f^2/v^2)$ constitutes effectively an $\mathcal{O}(v^2/f^2)$ contribution.

In order to include the box diagram with two T exchanges in our analysis one also has to calculate the $\mathcal{O}(v^4/f^4)$ corrections from the first two diagrams in Fig. 2, that have

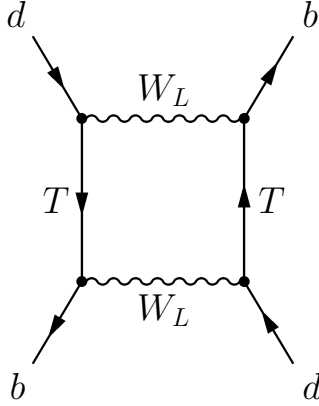


Figure 3: The dominant box diagram at $\mathcal{O}(v^4/f^4)$

to be taken into account in order to remove the divergences characteristic for a unitary gauge calculation and for the GIM mechanism [14] to become effective.

To this end the rules for the vertices in (2.9) and (2.10) have to be extended to the next order in v/f . Keeping only terms involving x_L , that are relevant for this discussion, let us write then

$$W_L^{+\mu\bar{t}}d_j = i\frac{g_2}{2\sqrt{2}} V_{tj} \left[1 - \frac{1}{2}x_L^2\frac{v^2}{f^2} + \left(d_1 + \frac{1}{2}ax_L^2\right)\frac{v^4}{f^4} \right] \gamma_\mu (1 - \gamma_5) \quad (5.2)$$

$$W_L^{+\mu\bar{T}}d_j = i\frac{g_2}{2\sqrt{2}} V_{tj} x_L \frac{v}{f} \left[1 + (d_2 - a)\frac{v^2}{f^2} \right] \gamma_\mu (1 - \gamma_5), \quad (5.3)$$

where the coefficients d_1 and d_2 could in principle be found by extending the analysis in [7] to include $\mathcal{O}(v^4/f^4)$ corrections. Fortunately, in order to find the dominant $\mathcal{O}(v^4/f^4)$ correction coming from the diagram in Fig. 3, the detailed knowledge of d_1 and d_2 turns out to be unnecessary. The reason is that in order to cancel all divergences or equivalently to satisfy the generalized unitarity relation in (2.18) at $\mathcal{O}(v^4/f^4)$, these two coefficients have to be related to each other as follows

$$d_1 = -d_2x_L^2 - \frac{x_L^4}{8}. \quad (5.4)$$

Indeed with (2.17) generalized to

$$\hat{V}_{tj} = V_{tj} \left(1 - \frac{x_L^2}{2}\frac{v^2}{f^2} + d_1\frac{v^4}{f^4} \right), \quad \hat{V}_{Tj} = V_{tj}\frac{v}{f}x_L \left(1 + d_2\frac{v^2}{f^2} \right) \quad (5.5)$$

the relation (2.18) is only satisfied at $\mathcal{O}(v^4/f^4)$, provided d_1 is related to d_2 as in (5.4).

Using this relation, the result for the sum of the diagram in Fig. 3 and the $\mathcal{O}(v^4/f^4)$ corrections from the first two diagrams in Fig. 2 can be written as

$$(\Delta S_t)_{TT} = \frac{v^4}{f^4} \left[x_L^4 P_{TT}(x_t, x_T) - 4(d_2 - 2a)x_L^2 P_1(x_t, x_T) \right] \quad (5.6)$$

with $P_1(x_t, x_T)$ given already in (4.10) and $P_{TT}(x_t, x_T)$ given simply as follows

$$P_{TT}(x_t, x_T) = F(x_T, x_T; W_L) + F(x_t, x_t; W_L) - 2F(x_t, x_T; W_L) . \quad (5.7)$$

The meaning of the functions $F(x_i, x_j; W_L)$ is as in the previous section. Exact formula for $P_{TT}(x_t, x_T)$ is given in the Appendix B.

As $P_1(x_t, x_T)$ increases only logarithmically with x_T , the second term in (5.6) is a genuine $\mathcal{O}(v^4/f^4)$ correction and can be safely neglected. On the other hand, the first term, that is independent of d_i , gives for $x_L \approx 1$

$$(\Delta S)_{TT} \approx \frac{v^4}{f^4} x_L^4 \frac{x_T}{4} = \frac{v^2}{f^2} \frac{x_L^3}{1-x_L} \frac{x_t}{4} . \quad (5.8)$$

Formula (5.8) represents for $x_L > 0.85$ and $f/v \geq 5$ the exact expression given in Appendix B to within 3% and becomes rather accurate for $x_L > 0.90$ and $f/v \geq 10$.

In fact the result in (5.8) can easily be understood. In the limit of a very large x_T it turns out to be a good approximation to evaluate $P_{TT}(x_t, x_T)$ with $x_t = 0$. In this case (5.7) reduces to $S_0(x_t)$ in (3.4) with x_t replaced by x_T and x_u by x_t . The factor $x_t/4$ in (5.1) is then replaced by $x_T/4$ as seen in (5.8).

The formula (5.8) and the exact expression for $P_{TT}(x_t, x_T)$ in Appendix B is the main result of this section.

6 Numerical Analysis

6.1 Input Parameters

We will now evaluate the size of the contributions ΔS_c , ΔS_t and ΔS_{ct} as given in Section 4. To this end we use the values of m_t and $M_{W_L^\pm}$ in (2.1) and the following ranges for the three new parameters

$$5 \leq f/v \leq 20, \quad 0 < x_L \leq 0.95, \quad 0.2 \leq s \leq 0.8. \quad (6.1)$$

This parameter space is larger than the one allowed by other processes [7]-[13] which typically imply $f/v \geq 10$ or even higher. But we want to demonstrate that even for f/v as low as 5, the corrections from LH contributions in this range of parameters, except for $x_L > 0.80$, are at most 20%.

6.2 The Size of the Corrections ($x_L \leq 0.8$)

Let us first analyze the size and the relative importance of the explicit $\mathcal{O}(v^2/f^2)$ corrections in (4.7) and of the W_H^\pm contribution represented by the last term in (4.7). We

denote them by ΔS_1 and ΔS_2 , respectively. Using the formulae (4.10) and (4.12) we have

$$\Delta S_1 = \frac{v^2}{f^2} \left[\frac{x_L^2}{2} x_t (\log x_T - 1.57) - 4a S_0(x_t) \right] \quad (6.2)$$

$$\Delta S_2 = 2 \frac{v^2}{f^2} x_t (1 - s^2)^2, \quad (6.3)$$

where we have used (2.3).

In Fig. 4 we show ΔS_1 and ΔS_2 as functions of v/f for different values of x_L and $s = 0.5$. For this value of s , ΔS_2 is significantly more important than ΔS_1 except for the largest x_L , where they are comparable and have the same sign. The inspection of the formulae (6.2) and (6.3) shows that for larger s and largest x_L , ΔS_1 can be more important than ΔS_2 , while for smaller s the dominance of ΔS_2 increases.

In Fig. 5 we show the ratio $\Delta S_t/S_0(x_t)$ as a function of v/f for different values of x_L and s . In this plot we have taken into account the correction in (4.18). This figure can be compared with the Fig. 2 of [19] demonstrating that the corrections to the SM expectations in the LH model found by us differ both in magnitude and sign from those found in [19]. We have also calculated the ratios $\Delta S_{ct}/S_0(x_c, x_t)$ and $\Delta S_c/S_0(x_c)$ to find that, in the whole range of parameters considered, they are below 0.03 and 0.02, respectively. In view of hadronic uncertainties in the evaluation of ΔM_K and ε_K that amount to at least 10%, the corrections ΔS_{ct} and ΔS_c can be neglected for all practical purposes.

We conclude therefore that

- The corrections from new contributions to ΔM_K , that is governed by $S_0(x_c)$, can be safely neglected.
- In the case of ε_K , ΔM_d and ΔM_s the new physics contributions enter to an excellent approximation universally only the function S_t but the observed enhancement in the range of parameters considered is by at most 20%.

6.3 The Region $x_L \approx 1$

Let us next investigate the size of corrections for $x_L \geq 0.8$ where the box diagrams with two T exchanges become important. In Fig. 6 we show (solid line)

$$(S_t)_{\text{tot}} = S_0(x_t) + \Delta S_t + (\Delta S)_{\text{TT}} \quad (6.4)$$

as a function of x_L for $f/v = 5$ and $f/v = 10$ and $s = 0.2$. The comparison with the results for ΔS_t obtained by means of the formulae of Section 4 (dashed lines) shows that for $x_L \geq 0.8$ the box diagrams with two T exchanges cannot be neglected and in fact

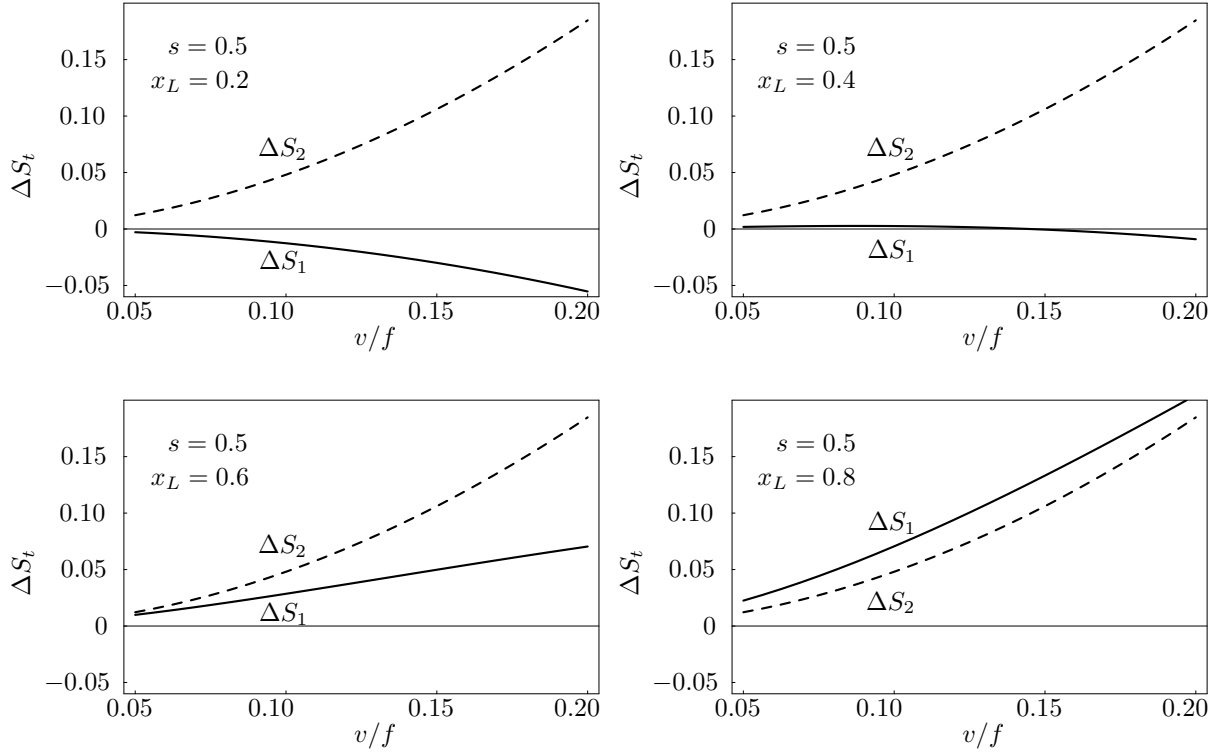


Figure 4: The Anatomy of Leading Contributions for $x_L \leq 0.8$.

for $x_L \geq 0.95$ they constitute the dominant correction. The total correction to the SM result amounts for $x_L = 0.95$ and $f/v = 5, 10$ to 56% and 15%, respectively. Additional numerical results can be found in [15].

6.4 Implications

The enhancement of the function S_t relative to $S_0(x_t)$, without the introduction of new operators and new complex phases beyond the KM phase is characteristic for all known models with minimal flavour violation (MFV) [34] like the MSSM at low $\tan\beta$ [35], and models with a single universal extra dimension [36]. Consequently, with the size of corrections found here for $x_L \leq 0.80$, it will be difficult to distinguish the Littlest Higgs model from other MFV models on the basis of particle-antiparticle mixing and ε_K alone. On the other hand for $x_L \geq 0.90$ a distinction could in principle be possible.

The size of the enhancement of S_t found here is for $x_L \leq 0.80$ comparable to the one present in models with a single universal extra dimension [36] but for $x_L > 0.90$ it is significantly larger and comparable with the maximal enhancements still allowed in the MSSM at low $\tan\beta$ [35]. Taking into account that in the LH model there are no new complex phases and the asymmetry $a_{\Psi K_S}$ measures the true angle β in the UT, the

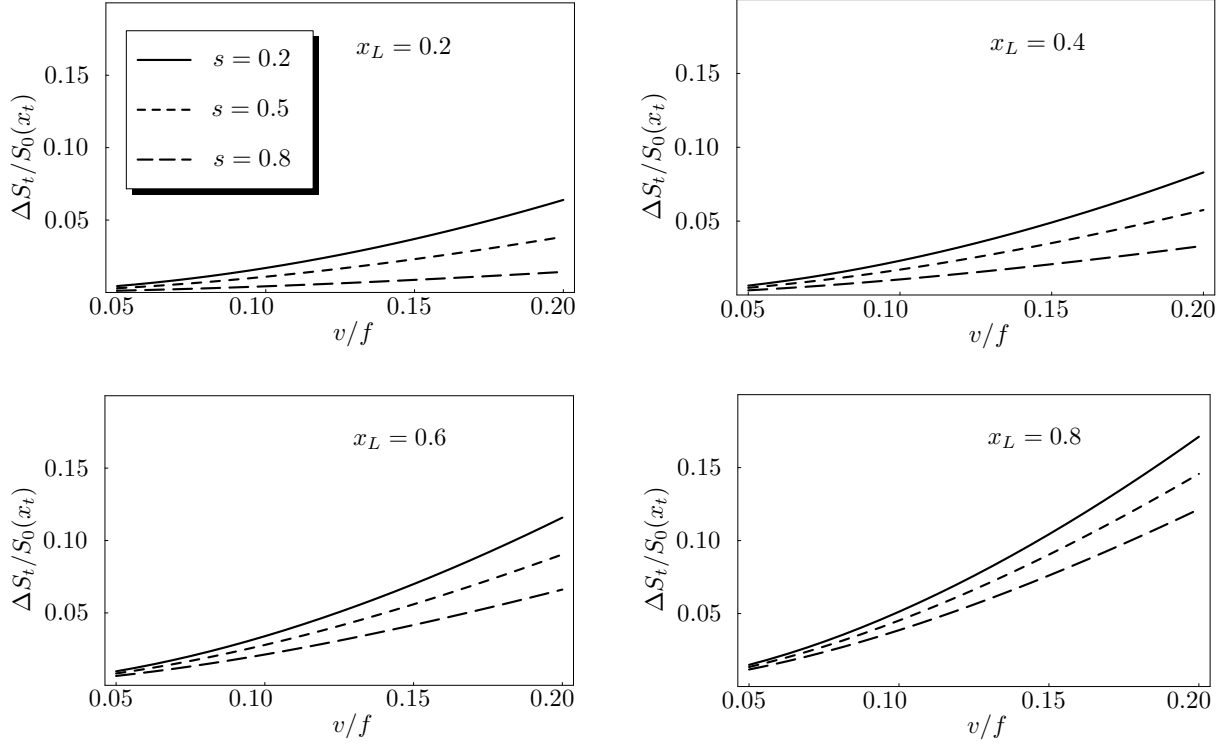


Figure 5: $\Delta S_t/S_0(x_t)$ versus v/f for different s and x_L

enhancement of S_t with respect to $S_0(x_t)$ in the SM implies through the formulae for ε_K and $\Delta M_{d,s}$ in (4.2) and (4.3)

$$(|V_{td}|)_{LH} < (|V_{td}|)_{SM}, \quad (R_t)_{LH} < (R_t)_{SM}, \quad \gamma_{LH} < \gamma_{SM}, \quad (\Delta M_s)_{LH} > (\Delta M_s)_{SM} \quad (6.5)$$

with R_t being the length of one of the sides of the UT. However, the suppressions and enhancements of these four quantities are at most by 15% for $v/f \leq 0.1$ as required by other processes. Such effects will be very difficult to detect unless the theoretical uncertainties in the relevant hadronic uncertainties will be decreased well below 5%. We have for instance

$$\frac{(R_t)_{LH}}{(R_t)_{SM}} = \sqrt{\frac{S_t}{S_0(x_t)}}, \quad \frac{(\Delta M_s)_{LH}}{(\Delta M_s)_{SM}} = \frac{S_t}{S_0(x_t)}, \quad (6.6)$$

where we have set the QCD corrections in the LH model and the SM to be equal to each other. We will discuss this issue in the next section.

In view of these findings, there is really no useful bound on f coming from the processes considered here when $x_L \leq 0.80$. A rough bound on f in this case turns out to be

$$f \geq 1 \text{ TeV} \quad (6.7)$$

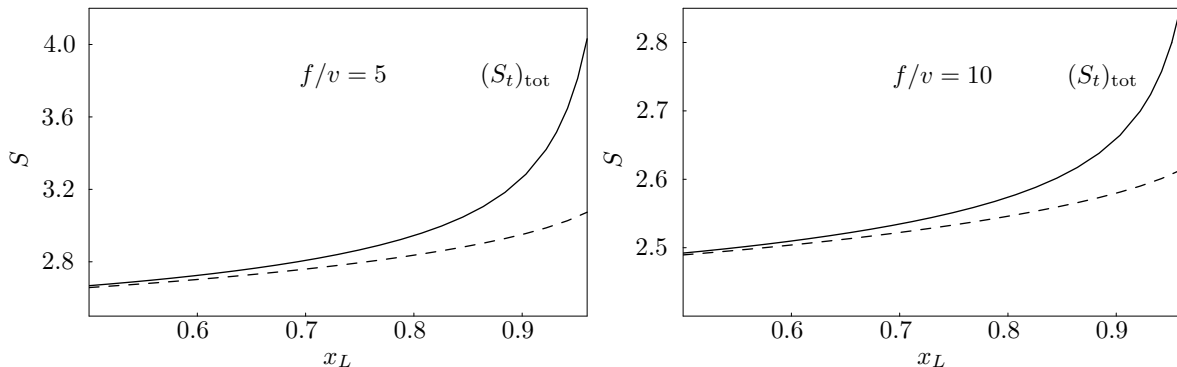


Figure 6: $(S_t)_{\text{tot}}$ (solid line) versus x_L for $s = 0.2$ and $f/v = 5, 10$. The dashed line represents the result without TT contribution. In the SM $S = S_0(x_t) = 2.42$.

that is weaker than the bound on f of 2 – 4 TeV found in analyses of electroweak precision observables [7, 8, 9, 10]. Only in the case of $x_L \geq 0.90$, some significant restrictions on the parameter space $(x_L, f/v)$ can in principle be obtained, provided the hadronic uncertainties present in $\Delta M_{s,d}$ will be considerably decreased. We refer to [15] for more details.

7 Comments on QCD Corrections

Until now our discussion assumed that the QCD factors η_i in (4.1) and (4.3) were the same for the SM and the LH model. In fact in the leading logarithmic approximation (LO) this would be true if all new heavy particles were $\mathcal{O}(m_t)$. Indeed at the LO what matters is only the renormalization group evolution of the $\Delta F = 2$ $(V - A) \otimes (V - A)$ operator that for scales below $\mu_t = \mathcal{O}(m_t)$ is the same in the SM and the LH model. At the next-to-leading level explicit $\mathcal{O}(\alpha_s)$ corrections to the diagrams of Fig. 2 enter, making the η_i factors in the SM and in the LH model differ by a small amount [29, 30, 37].

However integrating out simultaneously the heavy T , W_H^\pm and Φ^\pm and the significantly lighter t and W_L^\pm , as we have done by calculating the diagrams of Fig. 2, is certainly a rough approximation. Indeed assuming that T , W_H^\pm and Φ^\pm have masses of $\mathcal{O}(f)$, the correct inclusion of QCD corrections and summation of large logarithms would require the removal of T , W_H^\pm and Φ^\pm as explicit degrees of freedom at $\mu_f = \mathcal{O}(f)$ and of t and W_L^\pm at $\mu_t = \mathcal{O}(m_t)$. Our experience with the calculations of η_1 and η_3 [29] tells us that in the range $\mu_t < \mu < \mu_f$ new operators would enter the renormalization group analysis even in the case of the term λ_t^2 . Only after W_L^\pm and t have been integrated out at μ_t , would the only operator left in the effective theory be the one in (4.1).

A renormalization group analysis for scales $\mu_t < \mu < \mu_f$ is clearly involved and certainly far beyond the scope of our paper. Moreover, in view of the smallness of the corrections found by us, it is difficult to justify such an involved analysis. On the other hand the experience with the calculations of QCD corrections to the quantities considered within the SM [30, 29, 37] indicates that the inclusion of renormalization group effects in the range $\mu_t < \mu < \mu_f$ would likely suppress the LH corrections further. However, without a detailed analysis we cannot prove it at present. As for $\mu \geq m_t$, α_s runs very slowly, the renormalization group effects in the range $\mu_t \leq \mu \leq \mu_f$ with $\mu_f = \mathcal{O}(f)$ are not expected to change our main conclusions.

8 Conclusions

In this paper we have calculated first $\mathcal{O}(v^2/f^2)$ corrections to the SM expectations for ΔM_K , $\Delta M_{d,s}$ and ε_K in the Littlest Higgs model in the case $x_L \leq 0.8$. The analytic expressions for these corrections are given in (4.7) and (4.8) and the numerical results in Figs. 4 and 5. Our main findings for this range of x_L are as follows:

- The dominant new contributions come from box diagrams with (W_L^\pm, W_H^\pm) and ordinary quark exchanges that are strictly positive.
- The $\mathcal{O}(v^2/f^2)$ corrections to the usual box diagrams with two W_L^\pm and ordinary quark exchanges have to be combined with box diagrams with a single heavy T exchange for GIM mechanism to work and to cancel the divergences that appear when the calculation is done in the unitary gauge. These corrections turn out to be both negative and positive, dependently on the values of parameters involved, and are smaller than those coming from box diagrams with (W_L^\pm, W_H^\pm) exchanges except for x_L approaching 0.8 when they start to be important.
- The contributions of the heavy scalars Φ^\pm are negligible.
- The corrections to ΔM_K are negligible.
- The corrections to $\Delta M_{d,s}$ and ε_K are positive in the full range of parameters considered. This implies the suppression of $|V_{td}|$ and of the angle γ in the unitarity triangle and an enhancement of ΔM_s relative to the SM expectations.
- However even for f as small as 1 TeV, these effects amount to at most (15 – 20)% corrections and decrease below 5% for $f > 3 - 4$ TeV as required by other processes [7]–[13]. In view of non-perturbative uncertainties in the quantities considered it

will be very difficult to distinguish LH model from the SM on the basis of particle-antiparticle mixing and ε_K alone if $x_L \leq 0.8$.

Interestingly,

- the size of corrections increases for $x_L \approx 1$, where the diagrams with two T exchanges become dominant. The relevant expression is given in (5.8) and the numerical results in Fig. 6. Now the corrections are sufficiently large that the distinction from SM expectations for $|V_{td}|$, γ and ΔM_s could in principle be possible. The corresponding numerical analysis can be found in [15].

Finally,

- we have emphasized, that the concept of the unitarity triangle is still useful in the LH model, in spite of the $\mathcal{O}(v^2/f^2)$ corrections to the CKM unitarity involving only ordinary quarks. To this end the basic CKM parameters to be used are the uncorrected ones. This should be useful for future studies of rare decays.
- One message is, however, clear: if ΔM_s will be found convincingly below the SM expectations, the LH model will be ruled out independently of the value of f .

Our results differ significantly from the ones obtained in the published version of [19], where a significant suppression of ΔM_d has been found. Meanwhile, the authors identified errors in their calculation and confirmed our results of Section 4.

It will be interesting to see whether the LH contributions to theoretically clean rare decays like $K \rightarrow \pi\nu\bar{\nu}$ [38] will be easier to detect than in quantities considered here. This issue is briefly discussed in [15]. We will present a detailed analysis of rare decays, that is much more involved, in [16], where also the comparison with the analysis of [20] will be given.

Acknowledgements

We would like to thank Thorsten Ewerth, Wolfgang Hollik, Heather Logan and Felix Schwab for useful discussions. Special thanks go to an unknown referee of the first version of our paper who asked us to explain the non-decoupling of T at $\mathcal{O}(v^2/f^2)$. This led us to reconsider our calculation of the function S and to include the box diagrams with two T exchanges. In this context we thank also Andreas Weiler for useful discussions. The work presented here was supported in part by the German Bundesministerium für Bildung und Forschung under the contract 05HT4WOA/3 and by the German-Israeli Foundation under the contract G-698-22.7/2002.

A The Non-Leading Contributions

For completeness we give here non-leading contributions to ΔS_t , and ΔS_{ct} .

The explicit $\mathcal{O}(v^2/f^2)$ corrections in the vertices of the third diagram in Fig. 2 result in

$$(\Delta S_t)_{W_L W_H} = -8 \frac{v^2 c^2}{f^2 s^2} \left[\tilde{a} P_3(x_t, y) + \frac{1}{2} x_L^2 P_5(x_t, x_T, y) \right] \quad (\text{A.1})$$

$$(\Delta S_{ct})_{W_L W_H} = -8 \frac{v^2 c^2}{f^2 s^2} \left[\tilde{a} P_4(x_c, x_t, y) + \frac{1}{4} x_L^2 P_6(x_c, x_t, x_T, y) \right] \quad (\text{A.2})$$

with $(\Delta S_c)_{W_L W_H}$ obtained from (A.1) through the substitution $t \rightarrow c$. Here

$$\tilde{a} = \frac{a - b}{2} = \frac{(c^2 - s^2)^2}{4} \quad (\text{A.3})$$

with a and b defined in (2.14). The correction (4.18) contributes here at $\mathcal{O}(v^4/f^4)$. The functions $P_{3,4}$ are defined in Section 4 and $P_{5,6}$ are defined as follows

$$\begin{aligned} P_5(x_t, x_T, y) &= F(x_t, x_t, y; W_L, W_H) + F(x_u, x_T, y; W_L, W_H) \\ &\quad - F(x_t, x_T, y; W_L, W_H) - F(x_t, x_u, y; W_L, W_H) \end{aligned} \quad (\text{A.4})$$

$$\begin{aligned} P_6(x_c, x_t, x_T, y) &= F(x_c, x_t, y; W_L, W_H) - F(x_c, x_T, y; W_L, W_H) \\ &\quad - F(x_t, x_u, y; W_L, W_H) + F(x_T, x_u, y; W_L, W_H) \end{aligned} \quad (\text{A.5})$$

Explicit expressions for P_i are given in appendix B. We emphasize that these results include $\mathcal{O}(v^2/f^2)$ corrections to both W_L^\pm and W_H^\pm vertices, whereas in [19] only corrections to W_L^\pm vertices have been included. In that case $\tilde{a} = a/2$.

The contribution of the fourth diagram in Fig. 2 to ΔS_t reads

$$(\Delta S_t)_{W_L \Phi} = \frac{1}{2} \frac{v^2}{f^2} P_7(x_t, z) \quad (\text{A.6})$$

with P_7 given by

$$P_7(x_t, z) = F(x_t, x_t, z; W_L, \Phi) + F(x_u, x_u, z; W_L, \Phi) - 2F(x_t, x_u, z; W_L, \Phi) \quad (\text{A.7})$$

and z defined in (B.1). In obtaining (A.6) we have set the vacuum expectation value v' of the scalar triplet to zero.

We find that in the full range of parameters given in (2.3) one has

$$\frac{(\Delta S_t)_{W_L W_H}}{S_0(x_t)} \leq 3 \cdot 10^{-3}, \quad \frac{(\Delta S_{ct})_{W_L W_H}}{S_0(x_c, x_t)} \leq 3 \cdot 10^{-3}, \quad \frac{(\Delta S_t)_{W_L \Phi}}{S_0(x_t)} \leq 1 \cdot 10^{-3}. \quad (\text{A.8})$$

Consequently, all these contributions can be neglected.

B The Functions S_0 and P_i

In the following we list the functions S_0 and P_i that entered various formulae of our paper. We use

$$x_i = \frac{m_i^2}{M_{W_L^\pm}^2}, \quad y = \frac{M_{W_H^\pm}^2}{M_{W_L^\pm}^2}, \quad z = \frac{M_\Phi^2}{M_{W_L^\pm}^2}. \quad (\text{B.1})$$

$$S_0(x_t) = \frac{x_t(4 - 11x_t + x_t^2)}{4(-1 + x_t)^2} + \frac{3x_t^3 \log x_t}{2(-1 + x_t)^3} \quad (\text{B.2})$$

$$\begin{aligned} S_0(x_c, x_t) &= \frac{-3x_t x_c}{4(-1 + x_t)(-1 + x_c)} - \frac{x_t(4 - 8x_t + x_t^2)x_c \log x_t}{4(-1 + x_t)^2(-x_t + x_c)} \\ &+ \frac{x_t x_c(4 - 8x_c + x_c^2) \log x_c}{4(-1 + x_c)^2(-x_t + x_c)} \end{aligned} \quad (\text{B.3})$$

$$\begin{aligned} P_1(x_t, x_T) &= \frac{x_t(-4 + 11x_t - x_t^2 + x_T - 8x_t x_T + x_t^2 x_T)}{4(-1 + x_t)^2(-1 + x_T)} + \frac{x_t x_T(4 - 8x_T + x_T^2) \log x_T}{4(x_t - x_T)(-1 + x_T)^2} \\ &- \frac{x_t(-6x_t^3 - 4x_T + 12x_t x_T - 3x_t^2 x_T + x_t^3 x_T) \log x_t}{4(-1 + x_t)^3(x_t - x_T)} \end{aligned} \quad (\text{B.4})$$

$$\begin{aligned} P_2(x_c, x_t, x_T) &= \frac{3(x_t x_c - x_T x_c)}{4(-1 + x_t)(-1 + x_T)(-1 + x_c)} + \frac{(4x_t x_c - 8x_t^2 x_c + x_t^3 x_c) \log x_t}{4(-1 + x_t)^2(x_t - x_c)} \\ &+ \frac{(4x_t x_c^2 - 4x_T x_c^2 - 8x_t x_c^3 + 8x_T x_c^3 + x_t x_c^4 - x_T x_c^4) \log x_c}{4(x_t - x_c)(x_T - x_c)(-1 + x_c)^2} \\ &- \frac{(4x_T x_c - 8x_T^2 x_c + x_T^3 x_c) \log x_T}{4(-1 + x_T)^2(x_T - x_c)} \end{aligned} \quad (\text{B.5})$$

$$\begin{aligned} P_3(x_t, y) &= \frac{x_t(-4x_t + x_t^2 + 4y - 4x_t y)}{4(-1 + x_t)(x_t - y)y} + \frac{3x_t^3(x_t - 2y + x_t y) \log x_t}{4(-1 + x_t)^2(x_t - y)^2 y} \\ &- \frac{3x_t^2 y \log y}{4(x_t - y)^2(-1 + y)} \end{aligned} \quad (\text{B.6})$$

$$\begin{aligned} P_4(x_c, x_t, y) &= \frac{3x_c x_t y \log y}{4(x_t - y)(-1 + y)(y - x_c)} + \frac{(-4x_t + x_t^2 + 4y - 4x_t y)x_c x_t \log x_t}{4(-1 + x_t)(x_t - y)(x_t - x_c)y} \\ &- \frac{(-4y + 4x_c + 4yx_c - x_c^2)x_c x_t \log x_c}{4(-1 + x_c)(y - x_c)(x_t - x_c)y} \end{aligned} \quad (\text{B.7})$$

$$\begin{aligned}
P_5(x_t, x_T, y) &= -\frac{x_t(-3x_t^4 + 4x_t^2x_T - 2x_t^3x_T + x_t^4x_T + 6x_t^3y - 3x_t^4y - 8x_t x_T y) \log x_t}{4(-1+x_t)^2(x_t-x_T)(x_t-y)^2y} \\
&- \frac{x_t(+7x_t^2x_T y - 2x_t^3x_T y + 4x_T y^2 - 8x_t x_T y^2 + 4x_t^2x_T y^2) \log x_t}{4(-1+x_t)^2(x_t-x_T)(x_t-y)^2y} \\
&+ \frac{x_t x_T(-4x_T + x_T^2 + 4y - 4x_T y) \log x_T}{4(x_t-x_T)(-1+x_T)(x_T-y)y} + \frac{3x_t(x_t-x_T)y^2 \log y}{4(x_t-y)^2(x_T-y)(-1+y)} \\
&+ \frac{x_t(-4x_t + x_t^2 + 4y - 4x_t y)}{4(-1+x_t)(x_t-y)y} \tag{B.8}
\end{aligned}$$

$$\begin{aligned}
P_6(x_c, x_t, x_T, y) &= -\frac{x_c x_t(x_t^2 + 4y - 4x_t(1+y)) \log x_t}{4(x_c-x_t)(-1+x_t)(x_t-y)y} + \frac{x_c x_T(x_T^2 + 4y - 4x_T(1+y)) \log x_T}{4(x_c-x_T)(-1+x_T)(x_T-y)y} \\
&+ \frac{x_c^2(x_t-x_T)(x_c^2 + 4y - 4x_c(1+y)) \log x_c}{4(-1+x_c)(x_c-x_t)(x_c-x_T)(x_c-y)y} \\
&+ \frac{3x_c(x_t-x_T)y^2 \log y}{4(x_c-y)(-1+y)(-x_t+y)(-x_T+y)} \tag{B.9}
\end{aligned}$$

$$\begin{aligned}
P_7(x_t, z) &= \frac{x_t^2(-4+x_t)}{4(-1+x_t)(x_t-z)} - \frac{x_t^2(-3x_t^2 + 4z - 2x_t z + x_t^2 z) \log x_t}{4(-1+x_t)^2(x_t-z)^2} \\
&+ \frac{x_t^2(-4z + z^2) \log z}{4(x_t-z)^2(-1+z)} \tag{B.10}
\end{aligned}$$

$$\begin{aligned}
P_{TT}(x_t, x_T) &= \frac{x_T}{4} + \frac{-9 + 16x_t - 14x_t^2 + x_t^3}{4(-1+x_t)^2} - \frac{6}{4(-1+x_T)^2} - \frac{3(-5+3x_t)}{4(-1+x_t)(-1+x_T)} \\
&- \frac{x_t(-3x_t^3 - 4x_T + 12x_t x_T - 6x_t^2 x_T + x_t^3 x_T) \log x_t}{2(-1+x_t)^3(x_t-x_T)} \\
&+ \frac{x_T(-4x_t + 12x_t x_T - 6x_t x_T^2 - 3x_T^3 + x_t x_T^3) \log x_T}{2(x_t-x_T)(-1+x_T)^3} \tag{B.11}
\end{aligned}$$

References

- [1] N. Arkani-Hamed, A. G. Cohen and H. Georgi, Phys. Lett. B **513** (2001) 232 [arXiv:hep-ph/0105239].
- [2] N. Arkani-Hamed, A. G. Cohen, T. Gregoire and J. G. Wacker, JHEP **0208** (2002) 020 [arXiv:hep-ph/0202089].
- [3] N. Arkani-Hamed, A. G. Cohen, E. Katz, A. E. Nelson, T. Gregoire and J. G. Wacker, JHEP **0208** (2002) 021 [arXiv:hep-ph/0206020].

- [4] N. Arkani-Hamed, A. G. Cohen, E. Katz and A. E. Nelson, JHEP **0207** (2002) 034 [arXiv:hep-ph/0206021].
- [5] I. Low, W. Skiba and D. Smith, Phys. Rev. D **66** (2002) 072001 [arXiv:hep-ph/0207243].
- [6] M. Schmaltz, Nucl. Phys. Proc. Suppl. **117** (2003) 40 [arXiv:hep-ph/0210415].
H. E. Logan, arXiv:hep-ph/0307340.
H. E. Logan, Eur. Phys. J. C **33** (2004) S729 [arXiv:hep-ph/0310151].
- [7] T. Han, H. E. Logan, B. McElrath and L. T. Wang, Phys. Rev. D **67** (2003) 095004 [arXiv:hep-ph/0301040].
- [8] C. Csaki, J. Hubisz, G. D. Kribs, P. Meade and J. Terning, Phys. Rev. D **67** (2003) 115002 [arXiv:hep-ph/0211124].
- [9] J. L. Hewett, F. J. Petriello and T. G. Rizzo, JHEP **0310** (2003) 062 [arXiv:hep-ph/0211218].
- [10] M. C. Chen and S. Dawson, Phys. Rev. D **70** (2004) 015003 [arXiv:hep-ph/0311032]; arXiv:hep-ph/0409163.
- [11] C. x. Yue and W. Wang, Nucl. Phys. B **683** (2004) 48 [arXiv:hep-ph/0401214].
- [12] W. Kilian and J. Reuter, Phys. Rev. D **70** (2004) 015004 [arXiv:hep-ph/0311095].
- [13] T. Han, H. E. Logan, B. McElrath and L. T. Wang, Phys. Lett. B **563** (2003) 191 [arXiv:hep-ph/0302188].
- [14] S. L. Glashow, J. Iliopoulos and L. Maiani, Phys. Rev. D **2** (1970) 1285.
- [15] A. J. Buras, A. Poschenrieder and S. Uhlig, arXiv:hep-ph/0501230.
- [16] A. J. Buras, A. Poschenrieder and S. Uhlig, in preparation.
- [17] W. j. Huo and S. h. Zhu, Phys. Rev. D **68** (2003) 097301 [arXiv:hep-ph/0306029].
- [18] J. Y. Lee, arXiv:hep-ph/0408362.
- [19] S. R. Choudhury, N. Gaur, A. Goyal and N. Mahajan, Phys. Lett. B **601**, 164 (2004) [arXiv:hep-ph/0407050].
- [20] S. R. Choudhury, N. Gaur, G. C. Joshi and B. H. J. McKellar, arXiv:hep-ph/0408125.

- [21] C. Csaki, J. Hubisz, G. D. Kribs, P. Meade and J. Terning, Phys. Rev. D **68** (2003) 035009.
- [22] M. Perelstein, M. E. Peskin and A. Pierce, Phys. Rev. D **69** (2004) 075002.
- [23] S. Chang and J. G. Wacker, Phys. Rev. D **69** (2004) 035002 [arXiv:hep-ph/0303001].
- [24] S. Chang, JHEP **0312** (2003) 057 [arXiv:hep-ph/0306034].
- [25] L. Wolfenstein, Phys. Rev. Lett. **51** (1983) 1945.
- [26] A. J. Buras, M. E. Lautenbacher and G. Ostermaier, Phys. Rev. D **50** (1994) 3433 [arXiv:hep-ph/9403384].
- [27] M. K. Gaillard and B. W. Lee, Phys. Rev. D **10** (1974) 897.
- [28] A. J. Buras, arXiv:hep-ph/0307203.
- [29] S. Herrlich and U. Nierste, Nucl. Phys. B **419** (1994) 292 [arXiv:hep-ph/9310311]; Phys. Rev. D **52** (1995) 6505 [arXiv:hep-ph/9507262]; Nucl. Phys. B **476** (1996) 27 [arXiv:hep-ph/9604330].
- [30] A. J. Buras, M. Jamin and P. H. Weisz, Nucl. Phys. B **347** (1990) 491.
- [31] J. Urban, F. Krauss, U. Jentschura and G. Soff, Nucl. Phys. B **523** (1998) 40 [arXiv:hep-ph/9710245].
- [32] T. Inami and C. S. Lim, Prog. Theor. Phys. **65** (1981) 297 [Erratum-ibid. **65** (1981) 1772].
- [33] A. J. Buras, W. Slominski and H. Steger, Nucl. Phys. B **238** (1984) 529.
- [34] A. J. Buras, P. Gambino, M. Gorbahn, S. Jager and L. Silvestrini, Phys. Lett. B **500** (2001) 161 [arXiv:hep-ph/0007085]. G. D'Ambrosio, G. F. Giudice, G. Isidori and A. Strumia, Nucl. Phys. B **645** (2002) 155 [arXiv:hep-ph/0207036]. A. J. Buras, Acta Phys. Polon. B **34** (2003) 5615 [arXiv:hep-ph/0310208].
- [35] A. J. Buras, P. Gambino, M. Gorbahn, S. Jager and L. Silvestrini, Nucl. Phys. B **592** (2001) 55 [arXiv:hep-ph/0007313].
- [36] A. J. Buras, M. Spranger and A. Weiler, Nucl. Phys. B **660** (2003) 225 [arXiv:hep-ph/0212143].
- [37] G. Buchalla, A. J. Buras and M. E. Lautenbacher, Rev. Mod. Phys. **68** (1996) 1125 [arXiv:hep-ph/9512380].

[38] For the most recent review see A. J. Buras, F. Schwab and S. Uhlig, arXiv:hep-ph/0405132.